

Materials Analysis on a Microscale

Prospects for Trace Analysis in the Analytical Electron Microscope

D. B. Williams

Department of Materials Science and Engineering
Lehigh University
Bethlehem, PA 18015

Background

The analytical electron microscope (AEM) uses a high energy (≥ 100 kV) beam of electrons to generate a range of signals from a thin foil sample as shown in figure 1a [1,2]. Various detectors are configured in the AEM to pick up most of the generated signals (fig. 1b). Microanalysis is usually performed using the characteristic x-ray signal, detected by an energy dispersive spectrometer (EDS) although occasionally the electron energy loss spectrum is also used. This paper will emphasize x-ray microanalysis only. The specific advantages that the AEM has for microanalysis are two-fold. First the instrument can be operated as a high resolution transmission electron microscope, thus permitting the analytical information to be related directly to the microstructure of the sample. Second, in the AEM most microanalysis is performed with a probe size $< \approx 10$ nm and a specimen thickness $< \approx 100$ nm. This results in an analyzed volume $\approx 10^{-5}$ of that commonly encountered in bulk microanalysis, for example, in the electron probe microanalyzer (EPMA). This small volume means that the spatial resolution of microanalysis is relatively good (routinely < 50 nm) but generally trace analysis in the AEM is relatively difficult, because generated signal intensities are low.

X-Ray Microanalysis in the AEM

The definition of "trace analysis" in this paper is assumed to be that commonly used in the EPMA, namely elemental concentrations $< \approx 0.5$ wt% [3]. Under these conditions the average counts in

the x-ray characteristic peak, \bar{N} , approach the average counts in the background, \bar{N}^b .

One reasonable measure of analytical sensitivity used in the AEM field is the minimum mass fraction of one element that is detectable in the matrix of another. Using the criterion of Liebhafsky et al. [4], the peak is detectable if:

$$\bar{N} > 3(2\bar{N}^b)^{1/2} \quad (1)$$

This simple criterion can be combined with the Cliff-Lorimer equation [5] to give a minimum mass fraction of element B (C_B):

$$C_B = \frac{3(2I_B^b)^{1/2}}{I_A - I_A^b} \cdot C_A \cdot k_{AB}^{-1} \quad (2)$$

where I_A^b and I_B^b are background intensities for elements A and B; I_A is the integrated characteristic intensity from A; C_A is the concentration of A (in wt%) and k_{AB}^{-1} is the reciprocal of the Cliff-Lorimer sensitivity k -factor k_{AB} [5]. The equation can be rewritten [6] as:

$$C_B = \frac{3(2I_B^b)^{1/2}}{I_B - I_B^b} \cdot C_B \quad (3)$$

Results using eqs (2) and (3) have been given by Romig and Goldstein [7] ($\approx 0.5\%$ Ni in Fe), Michael [6] ($\approx 0.07\%$ Mn in Cu) and Lyman [8] ($\approx 0.1\%$ Ni in Fe). The results of Michael [6] are shown in table 1. What is not apparent in these reported values is that since all the data were obtained from homogeneous samples, spatial resolution was of little consequence and was usually > 50 nm which is the current limit for most thermionic source AEMs. The data in table 2 [9] are the first to compare the effect of spatial resolution on minimum detectability. These results show that a sensitivity < 0.1 wt% Cr with moderate spatial resolution ($< \approx 50$ nm) can only be achieved with an AEM employing a field emission gun, such as the Vacuum Generators HB501. Thermionic source instruments such as the Philips EM430 can only demonstrate < 0.1 wt% detectability with substantially poorer spatial resolution.

Table 1. Calculation of the minimum mass fraction of Mn detectable in Cu using eq (3)

I_{Mn}	I_{Mn}^b	$(I_{Mn} - I_{Mn}^b)$	$3(2I^b)$	$C_{Mn}(MMF) = C_{Mn} \times \frac{3(2I^b)}{(I_{Mn} - I_{Mn}^b)} \text{ wt\%}$
11904	1995 ± 189	9909 ± 422	189 ± 9	0.064 ± 0.008
13769	2299 ± 203	11470 ± 454	203 ± 9	0.059 ± 0.007
10737	1860 ± 183	8877 ± 400	183 ± 9	0.069 ± 0.008
10547	1916 ± 186	8631 ± 394	186 ± 9	0.072 ± 0.009
				av. = 0.067 ± 0.008 wt%

Specimen Cu 3.36 wt% Mn.

Data obtained at 120 kV, 20 nm probe size, 40 μA emission current, 70 μm C₂ aperture, W hairpin filament.

From refs [1,7]. Reproduced courtesy of Philips Electronic Instruments Publishing Group.

Table 2. Calculated MMF values for Cr after 200 s livetime and spatial resolution of microanalysis for a range of AEMs

Microscope	Probe current (nA)	Accelerating voltage (kV)	Sample Thickness (nm)	Cr MMF wt%	Calculated spatial resolution (nm)
HB-501	0.5	100	164	0.125	45
HB-501	1.7	100	164	0.069	45
HB-501	0.5	100	434	0.056	200
HB-501	1.7	100	434	0.035	200
EM430	0.5	100	164	0.181	70
EM430	0.8	300	164	0.135	25
EM430	0.5	100	434	0.054	200
EM430	0.8	300	434	0.053	70

Data from ref. [8]. Reproduced by permission of C. E. Lyman and San Francisco Press.

Future Prospects for X-Ray Analysis in the AEM

However, recent instrumental developments promise substantial improvement in trace analysis capability in the AEM. A combination of higher voltage beams (up to 400 kV), brighter (field emission) electron sources, improved microscope stage design [10] and x-ray spectrometry advances offer the prospect of extending the minimum mass fraction detectable by x-ray analysis down to ≈0.01 wt% [8]. If this can be achieved while maintaining spatial resolution at the 10 nm level or below, then the AEM will be close to detecting the presence of only a few atoms, as well as localizing them to within a few tens of unit cells.

From an experimental standpoint, Ziebold [11] has shown that C_B depends on several factors, namely:

$$C_B \propto (I_B \cdot I_B / I_B^b \cdot \tau)^{-1/2} \quad (4)$$

where τ is the counting time to acquire the peak. Going to an intermediate voltage such as 300 kV,

will increase the value of I_B (the peak intensity) and I_B / I_B^b (the peak to background ratio (P/B)) [8]. Unfortunately, there is no generally accepted definition of P/B . A recent attempt has been made to generate a "standard" sample from which to measure a "standard" P/B [12,13].

The standard sample is a 100 nm of evaporated Cr on a carbon film, supported on a Cu grid, and manufactured at the National Bureau of Standards.¹ The value of the P/B used is that originally suggested by Fiori et al. [14] and ratios the intensity in the full peak to the average background in a 10 eV channel. Thus the ratio is defined as P/B (10 eV).

Preliminary results (table 3) [13] indicate that modern AEMs show an enormous range in P/B (10 eV) at 100 kV and not all intermediate voltage instruments show the expected improvement at higher kVs. Nevertheless, an improved M_{DL} of ≈0.05 wt% in a 10 nm probe is estimated at

¹ Standard films may be obtained from Dr. E. B. Steel, Analytical Chemistry Division, Bldg. 222, Room A121, National Bureau of Standards, Gaithersburg, MD 20899.

Accuracy in Trace Analysis

300 kV. However, if an FEG were added to a 300 kV AEM, a probe current of 5×10^{-8} to 10^{-7} A should be available in a 10 nm probe. This increase in probe current would result in an increase in P of 100 times and would improve the M_{DL} by ≈ 10 times to 0.01 wt% in a nominal 100 to 200 nm thick film at 300 kV [8]. Such an improvement of over an order of magnitude in analytical sensitivity brings x-ray analysis in the AEM into the 100 ppm range similar to that obtained in the electron probe microanalyzer. None of these calculations takes into account the possibility of increasing the value of τ in eq (4). Typically τ is limited by contamination, specimen drift and operator fatigue. Contamination can be virtually eliminated by careful specimen preparation and good ($< 10^{-8}$ Torr) vacuums. Specimen drift can now be compensated electronically [15], effectively eliminating operator fatigue and permitting such experiments as overnight counting, long-term digital mapping and other techniques, hitherto the realm of classical bulk analysis using the EPMA at the micron level.

Table 3. Peak to background (P/B (10 eV)) data for the CrK_{α} peak obtained from a standard thin film sample in a range of AEMs

AEM	kV	α°	Ω (sr)	P/B
1	120	20	0.13	1621
2	100	20	0.13	3346
2	200	20	0.13	3181
2	300	20	0.13	2991
3	300	25	0.13	2983
4	100	20	0.13	3177
5	200	72	0.03	2489
6	200	72	0.01	2873
7	100	10	0.02	3007
7	100	13	0.077	2690
8	100	13	0.077	3120
9	120	20	0.13	2879
10	100	30	0.13	2255
11	100	25	0.04	3040
12	200	34	0.005	2300
12	200	37	---	3300
13	120	20	0.13	3093

Reproduced courtesy of San Francisco Press.
 α° = detector take-off angle above horizontal.
 Ω = detector solid angle.

Acknowledgments

The author wishes to acknowledge the financial support of the National Aeronautics and Space Administration (NASA Grant NAG9-45) and many stimulating discussions with C. E. Lyman and J. R. Michael.

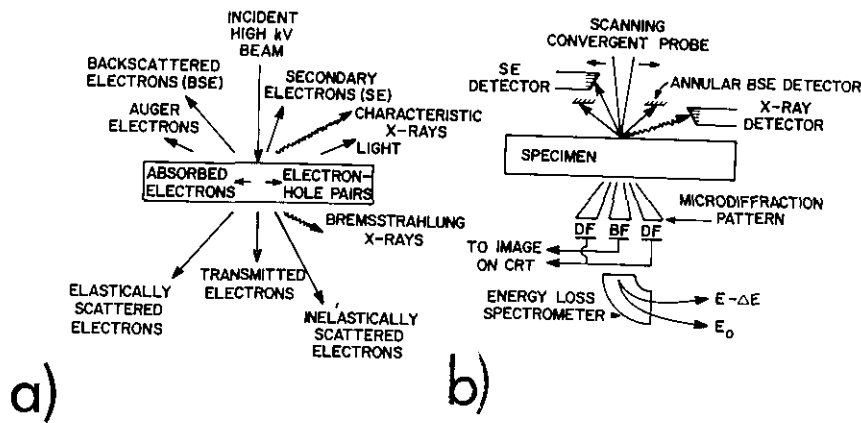


Figure 1. a. Schematic diagram showing the range of signals generated when a high kV electron beam strikes a thin foil sample.
 b. Typical array of detectors in a modern analytical electron microscope.

References

- [1] Williams, D. B., *Practical Analytical Electron Microscopy in Materials Science*, Philips Electron Optics Publishing Group, Mahwah, NJ (1984).
- [2] Joy, D. C., Romig, A. D., and Goldstein, J. I., *Principles of Analytical Electron Microscopy*, Plenum Press, New York (1986).
- [3] Goldstein, J. I., Newbury, D. E., Echlin, P., Joy, D. C., Fiori, C. E., and Lifshin, E., *Scanning Electron Microscopy and X-ray Microanalysis*, Plenum Press, New York (1981) p. 435.
- [4] Liebhafshy, H. A., Pfeiffer, H. G., and Zeman, P. D., *X-ray Microscopy and X-ray Microanalysis*, Elsevier/North Holland, Amsterdam (1960) p. 321.
- [5] Cliff, G., and Lorimer, G. W., *J. Microsc. (U.K.)* **103**, 203 (1975).
- [6] Michael, J. R., M.S. Thesis, Lehigh University (1981) p. 41.
- [7] Romig, A. D., and Goldstein, J. I., *Detectability Limits and Spatial Resolution in STEM X-ray Analysis: Application to Fe-Ni Alloys*, Microbeam Analysis—1979, San Francisco Press (1979) p. 124.
- [8] Lyman, C. E., *Microanalysis Limits on the Use of Energy Dispersive X-ray Spectroscopy in the Analytical Electron Microscope*, Microbeam Analysis—1986, San Francisco Press (1986) p. 434.
- [9] Lyman, C. E., and Michael, J. R., *A Sensitivity Test for Energy Dispersive X-ray Spectrometry in the Analytical Electron Microscope*, Analytical Electron Microscopy—1987, San Francisco Press (1987) in press.
- [10] Williams, D. B., *Towards the Limits of Microanalysis in the Analytical Electron Microscope*, Electron Microscopy and Analysis—1987, The Institute of Physics (1987) in press.
- [11] Ziebold, T. O., *Anal. Chem.* **36**, 322 (1967).
- [12] Williams, D. B., *Standardized Definitions of X-ray Analysis Performance Criteria in the AEM*, Microbeam Analysis—1986, San Francisco Press (1986) p. 443.
- [13] Williams, D. B., and Steel, E. B., *A Standard Cr Thin Film Specimen to Measure the X-ray Peak to Background Ratio (Using the Fiori Definition) in Analytical Electron Microscopes*, Analytical Electron Microscopy—1987, San Francisco Press (1987) in press.
- [14] Fiori, C. E., Swyt, C. R., and Ellis, J. R., *The Theoretical Characteristic to Continuum Ratio in Energy Dispersive Analysis in the Analytical Electron Microscope*, Microbeam Analysis—1982, San Francisco Press (1982) p. 57.
- [15] Vale, S. H., and Statham, P. J., *STEM Image Stabilization for High Resolution Microanalysis*, Proc. XIth Int. Cong. on Electron Microscopy, Kyoto 1986, Japanese Society of Electron Microscopy, Tokyo (1986) p. 573.

Accuracy in Microanalysis by Electron Energy-Loss Spectroscopy

Ray F. Egerton

Department of Materials Science and Engineering
State University of New York
Stony Brook, NY 11794-2275

The transmission electron microscope can focus electrons onto a small region of a specimen, typically 1 nm to 1 μ m in diameter. If the specimen is suitably thin (preferably < 100 nm) and the transmitted electrons enter a high-resolution electron spectrometer, an electron energy-loss spectrum is produced. This spectrum (fig. 1) contains a zero-loss peak, representing elastic scattering, one or more peaks in the 4–40 eV range (due to inelastic scattering from outer-shell electrons) and, at higher energy loss and lower intensity, characteristic edges due to ionization of inner atomic shells. These latter features are used in elemental microanalysis, usually by fitting a background in front of each edge and measuring the area I_c over an energy range Δ beyond each edge; see figure 1. The number of atoms (N per unit specimen area) of a particular element can be obtained from [1]:

$$N \approx I_c / G I_1 \sigma_c \quad (1)$$

The factor G makes allowance for any increase in detector gain between recording the low-loss region (area I_1) and the ionization edges; σ_c is a cross section for inner-shell scattering over the appropriate range of energy loss, which can be calculated from atomic theory or obtained experimentally. Energy-loss spectroscopy is therefore capable of providing absolute, standardless elemental analysis, although in practice it is usually the ratio of two elements which is of interest, in which case the quantities G and I_1 cancel and need not be measured.

Energy-loss spectroscopy has been used to identify quantities of less than 10^{-20} g and concentrations of less than 100 ppm of elements such as phosphorus and calcium in an organic matrix [2,3]. However, the accuracy of quantitative analysis, using eq (1), is often no better than 20%. The main sources of error, and possibilities for their removal, are discussed below.